https://doi.org/10.46389/rjd-2026-2197
www.rjdnmd.org

Rom J Diabetes Nutr Metab Dis
2026; volume 33, issue 2, pages 214–224

Original Article

Morphometric characteristics of the vascular bed in the rectus abdominis muscle during correction of diabetic myopathy with mesenchymal stem cells

Myroslav Kritsak [1] *, Serhiy Konovalenko [2], Oleh Kuziv [3], Oleh Yasinovskyi [3]

[1] Department of Surgery, I. Horbachevsky Ternopil National Medical University, Ternopil, Ukraine
[2] Department of Descriptive and Clinical Anatomy, Bogomolets National Medical University, Kyiv, Ukraine
[3] Department of Operative Surgery and Clinical Anatomy, I. Horbachevsky Ternopil National Medical University, Ternopil, Ukraine

* Correspondence to: Myroslav Kritsak, Department of Surgery, I. Horbachevsky Ternopil National Medical University, Ternopil, Ukraine. Phone: +380977602596; E-mail: kricakmy@gmail.com

Received: 10 April 2026 / Accepted: 2 June 2026

Abstract

The aim of the study was to analyze the morphometric characteristics of the vascular bed in the rectus abdominis muscle and to evaluate the therapeutic efficacy of mesenchymal stem cell therapy in an experimental model of type 2 diabetes. The study was conducted on 30 rats divided into three groups: control, untreated diabetes, and diabetes treated with MSCs. Morphometric, histological, and statistical methods were employed. It was established that the progression of diabetes is accompanied by inward hypertrophic remodeling of the arteries: the Voganworth index increased to (38.5±3.41) %, while the vascular lumen narrowed to (18.9±1.23) μm. Significant endothelial destruction (31.6±3.40) % and mucoid swelling of the vascular wall were observed. The administration of MSCs led to a significant correction of the metabolic profile and initiated reverse remodeling processes. In the MSC-treated group, there was an expansion of the arterial lumen, a reduction in media thickness to (5.53±0.46) μm, and a 2.6-fold decrease in the volume of endothelial damage compared to the untreated diabetic group. Histological analysis confirmed the stabilization of the connective tissue matrix and regression of vascular wall edema under the influence of cell therapy. Mesenchymal stem cells exhibit a pronounced angioprotective effect, restoring the microvascular architecture and improving tissue insulin sensitivity, which highlights their potential for the treatment of diabetic myopathy.

Keywords: type 2 diabetes mellitus, metabolic syndrome, microangiopathy, insulin resistance, skeletal muscle, regenerative medicine

Introduction

Type 2 diabetes mellitus (T2DM) remains one of the most pressing medical and social challenges of the 21st century, reaching the proportions of a global non-communicable disease epidemic. According to the International Diabetes Federation (IDF), the prevalence of this pathology is steadily increasing, which is accompanied by a high risk of long-term disability [1]. One of the less explored yet clinically significant complications of T2DM is diabetic myopathy, characterized by progressive loss of muscle mass, reduced muscle strength, and degenerative alterations in skeletal muscle architecture [2, 3].

Traditionally, research focus has been primarily directed toward diabetic neuropathy and lower extremity angiopathy. However, contemporary data highlight the existence of a specific phenomenon, diabetic myopathy. Chronic hyperglycemia triggers a cascade of metabolic disturbances, where the accumulation of

advanced glycation end products plays a pivotal role. These compounds modify the basement membrane proteins of capillaries and arterioles, leading to basement membrane thickening and profound endothelial dysfunction [4, 5].

It is crucial to consider that skeletal muscle serves as the primary site for glucose disposal in both humans and animals. Under physiological metabolic conditions, approximately 75–80% of postprandial glucose is cleared by skeletal muscle via insulin-dependent GLUT4 transporters [6]. However, in T2DM, a cascade of pathological alterations occurs, leading to a reduction in capillary bed density and impaired muscle perfusion [7]. This structural degradation physically limits the delivery of insulin and glucose to myocytes. Consequently, skeletal muscle microangiopathy should be regarded not merely as a secondary complication, but as a fundamental driver that exacerbates insulin resistance [8].

Skeletal muscle functions as an endocrine organ, secreting various biologically active substances known as myokines. In the context of diabetic muscle damage, the secretory balance of these factors is profoundly disturbed. A reduction in the secretion of vasoprotective myokines exacerbates endothelial dysfunction systemicly, transforming the management of diabetic myopathy into a critical target for general internal medicine [9].

In recent decades, research has pivoted toward mesenchymal stem cells (MSCs) as a versatile tool in regenerative medicine. MSCs possess a unique homing ability to migrate to sites of injury and exhibit potent paracrine activity. They secrete a broad spectrum of angiogenic factors, including vascular endothelial growth factor (VEGF), fibroblast growth factor (FGF), and insulin-like growth factor-1 (IGF-1), which stimulate endothelial cell proliferation and restore vascular wall integrity [10, 11]. However, the efficacy of cell therapy is heavily contingent upon the delivery route. Conventional intravenous administration is frequently hindered by the "pulmonary first-pass effect" (pulmonary filter), where up to 80% of transplanted cells are sequestered in the lungs [12]. In the present study, we utilized the intracardiac injection technique, which bypasses the pulmonary circulation and delivers cells directly into the systemic arterial bed. This approach ensures maximum bioavailability of MSCs to the skeletal muscle microvasculature.

The investigation of these pathological processes in humans is constrained by ethical standards and the inherent difficulty of obtaining serial biopsy material at various disease stages. Consequently, the utilization of a long-term rat model, combining a high-fat diet (HFD) with low-dose streptozotocin (STZ) induction, provides a robust approximation of the clinical course of T2DM in humans. This experimental paradigm enables the assessment of not only the acute effects of hyperglycemia but also the chronic vascular remodeling that typically evolves over an extended period.

The aim of this study was to determine the morphometric characteristics of small-caliber arteries in the rectus abdominis muscle during the treatment of diabetic myopathy with mesenchymal stem cells and to evaluate their impact on systemic insulin resistance.

Material and methods

The study was conducted on 30 male Wistar rats, aged 8 months. All experimental procedures were performed in strict accordance with the ethical principles of animal experimentation, adhering to the provisions of the European Convention for the Protection of Vertebrate Animals used for Experimental and Other Scientific Purposes (Strasbourg, 18.03.1986), the Directive 2010/63/EU of the European Parliament and of the Council on the protection of animals used for scientific purposes, and the Law of Ukraine "On the Protection of Animals from Cruelty."

Experimental animals were divided into three groups (n=10 per group). The control group (CG) consisted of healthy rats with a mean body weight of (220.00±15.00) g. In the second (HFD+DM) and third (HFD+DM+MSC) groups, a high-fat diet (HFD) was initiated from one month of age to induce obesity. The dietary regimen was formulated such that animal fats accounted for 30–60% of the total caloric intake. To enhance palatability and ensure consistent consumption, the daily ration per individual was supplemented with bread (6.0 g), pearl barley (4.0 g), barley (15.0 g), and carrots (10.0 g), along with a crushed mixture of sunflower seeds, peanuts, and oilcake. At the end of the dietary induction period, the body weights in the HFD+DM (429.62±23.45) g and HFD+DM+MSC (421.42±20.36) g groups showed no significant difference between each other but were significantly higher compared to the CG ($p<0.001$).

In the 7th month of the experiment, T2DM was induced in the HFD+DM and HFD+DM+MSC groups by a single intraperitoneal injection of streptozotocin (STZ) 35 mg/kg body weight dissolved in 0.1 M citrate buffer (pH 4.5). Prior to STZ administration, animals were

fasted for 12 hours with ad libitum access to water. Both groups continued the high-fat diet for an additional month (until the end of the 8th month). In the HFD+DM+MSC group, on the 7th day post-STZ induction, MSCs were administered via intracardiac injection at a dose of 1×10^6 cells suspended in 0.2 ml of isotonic saline 0.9% NaCl. The procedure was performed under general anesthesia induced by intraperitoneal ketamine 90 mg/kg and xylazine 10 mg/kg. The MSC suspension was slowly infused into the left ventricular cavity using a fine-gauge needle, guided by anatomical landmarks to ensure systemic arterial distribution [13].

The development of T2DM was confirmed by measuring blood glucose levels from the tail vein using an Accu-Chek glucometer (Roche Diagnostics, Germany) and by the presence of persistent hyperglycemia. To evaluate insulin sensitivity, an insulin tolerance test (ITT) was performed at the end of the 8th month. Insulin was administered intraperitoneally at a dose of 0.75 U/kg, with blood glucose levels measured at 0, 30, 60, 90, and 120 minutes post-injection.

Human umbilical cord-derived mesenchymal stem cells were isolated and characterized at the Cell Culture Laboratory of I. Horbachevsky Ternopil National Medical University. The umbilical cord tissue was obtained from a healthy donor following an uncomplicated physiological pregnancy and natural delivery, after obtaining informed consent for the use of postpartum biological material. The primary culture of MSCs was isolated from Wharton's jelly using an enzymatic digestion method with 0.1% collagenase type I (Sigma-Aldrich, USA). The cells were cultured in DMEM/F12 Advanced medium (Gibco, USA) supplemented with 10% fetal bovine serum (FBS) (Gibco, USA) at 37°C in a humidified atmosphere with 5% CO_2. Passaging was performed using TrypLE Express Enzyme (Gibco, USA). MSCs were cryopreserved at the 4th passage in a cryoprotective medium consisting of 30% DMEM/F12 Advanced, 40% FBS, 20% conditioned medium, and 10% dimethyl sulfoxide (DMSO, Sigma, USA). For the experimental studies, 5th passage MSCs were used. After thawing, cells were re-cultured under standard conditions. The MSC suspension was prepared using physiological saline 0.9% NaCl. To ensure maximum viability, the cell suspension was administered within 3 hours of detachment from the culture flasks.

The choice of intracardiac administration (specifically into the left ventricular cavity) was dictated by the necessity to maximize the systemic bioavailability of the MSCs within the arterial bed, following a critical evaluation of alternative delivery routes. Conventional systemic venous administration results in a significant proportion of MSCs (up to 80%) being sequestered in the pulmonary capillary network (the "pulmonary first-pass effect"), which drastically limits the number of viable cells reaching target tissues. Direct injection into the left ventricle bypasses pulmonary sequestration, ensuring immediate distribution throughout the systemic circulation a factor critical for the effective management of microangiopathies. The intraperitoneal route was excluded due to the low rate of cellular absorption into the systemic bloodstream and potential inactivation within the abdominal mesothelium. Local injections directly into the m. rectus abdominis were deemed inappropriate, as they induce additional mechanical trauma to already degenerated muscle tissue and fail to address the systemic vascular disturbances that are the primary etiology of diabetic myopathy. Thus, left ventricular puncture using a fine-gauge (insulin) needle achieved direct contact between the stem cells and the endothelium of small-caliber arteries under physiological pressure, while minimizing the volume of injected fluid and maintaining high animal survival rates.

The selection of the rectus abdominis muscle as the primary object of study was based on several critical factors. This muscle is a classic skeletal muscle with a predominance of type II (fast-twitch) fibers, which exhibit high sensitivity to both insulin action and ischemic injury. Consequently, data obtained from this model can be reliably extrapolated to the trunk musculature, which typically undergoes accelerated atrophy during the progression of diabetes. Furthermore, the rectus abdominis possesses a distinct anatomical localization and a strictly parallel fiber orientation. This structural consistency allows for the preparation of highly standardized cross-sections, which is essential for precise and reproducible morphometric measurements. From a hemodynamic perspective, the rectus abdominis is supplied by the epigastric artery system, which are direct branches of major systemic vessels. Given the intracardiac route of MSC administration, this ensures efficient delivery of the cells from the aorta into the microvascular bed of the target muscle under optimal perfusion conditions.

Upon completion of the experiment, tissue samples from the right rectus abdominis muscle were harvested and fixed in a 10% neutral buffered formalin solution. Following a standardized dehydration protocol in a graded series of alcohols, the specimens were embedded in paraffin blocks. Histological sections

 https://doi.org/10.46389/rjd-2026-2197

5–7 µm thick were prepared using a microtome. After deparaffinization, the sections were stained with hematoxylin and eosin, Masson's trichrome (to evaluate connective tissue), and Alcian blue (to detect mucoid swelling and glycosaminoglycans).The morphometric analysis of small-caliber arteries within the muscle tissue was conducted using specialized image analysis software. The following parameters were evaluated: external and internal vascular diameters (µm); tunica media thickness (µm); media-to-lumen ratio, also referred to as the Voganworth index (calculated as the ratio of the media thickness to the lumen diameter, expressed as a percentage); endothelial cell height (µm); nuclear-cytoplasmic ratio in endothelial cells; relative volume of damaged endothelial cells (%).

Statistical analysis of the obtained data was performed using STATISTICA 10.0 software (StatSoft, USA). The normality of the data distribution was verified using the Shapiro-Wilk test. For normally distributed data, intergroup differences were assessed using the parametric Student's t-test for independent samples. The results are expressed as the arithmetic mean±standard deviation (M±SD). To compare mean values across the three groups, one-way analysis of variance (ANOVA) was employed, followed by the Tukey post-hoc test for multiple comparisons. Correlations between morphometric parameters were assessed using the Pearson correlation coefficient (r) for normally distributed data or the Spearman rank correlation coefficient (ρ) for non-normally distributed data. Differences were considered statistically significant at $p<0.05$.

Results

Analysis of the glycemic curves during the ITT revealed significant disparities in metabolic responses across the experimental groups (Figure 1). In the HFD+DM group (untreated diabetes), a pathological curve profile was observed, characteristic of pronounced systemic insulin resistance. Despite the administration of exogenous insulin, blood glucose levels remained persistently elevated throughout the testing period. At the 60th minute, the glycemic reduction was only 15.6% from the baseline, which differed significantly from the control group ($p<0.001$). The administration of MSCs in the HFD+DM+MSC group led to a substantial modification of the metabolic profile. A dynamic decrease in glucose levels was recorded as early as the 30th minute, reaching a nadir at the 60th minute (6.69±0.68) mmol/L. This shift indicates a partial restoration of peripheral insulin sensitivity, particularly within skeletal muscle tissue. Glycemic values in the HFD+DM+MSC group at the 30, 60, and 90-minute marks were significantly lower than those in the HFD+DM group ($p<0.001$ according to Tukey's post-hoc test), confirming the high therapeutic efficacy of the intracardiac cell delivery method. By the end of the test (120 min), the MSC group exhibited a gradual recovery of glucose levels, reflecting the physiological termination of insulin action and the adequate engagement of counter-regulatory mechanisms.

The restoration of insulin sensitivity following MSC administration correlates with the improvement of morphometric parameters within the muscle

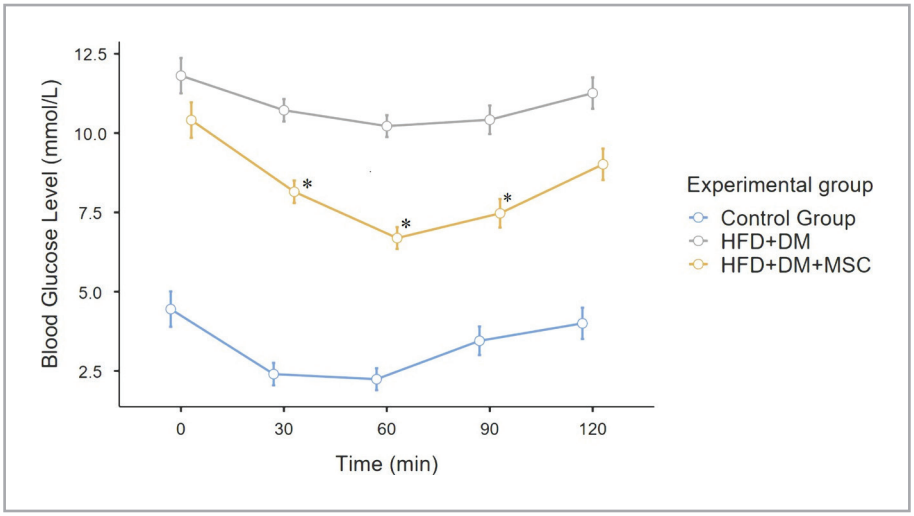

Figure 1: Dynamic changes in blood glucose levels during the insulin tolerance test. CG – Control Group; HFD+DM – High-Fat Diet and Streptozotocin-induced diabetes group; HFD+DM+MSC – group treated with mesenchymal stem cells via intracardiac injection. Data are presented as M±SD. * – $p<0.001$ compared to the HFD+DM group.

microcirculatory bed. Our morphometric analysis of the small-caliber arteries in the rectus abdominis muscle revealed profound structural disorganization of the vascular wall under conditions of long-term T2DM induced by a high-fat diet (Table 1). In the control group (CG), the external diameter of the arteries was (34.2±1.07) μm. The development of T2DM against the background of alimentary obesity did not lead to significant changes in the total arterial caliber, which measured (33.5±1.04) μm in the HFD+DM group ($p=0.358$ *vs.* CG). A similar trend was observed in the HFD+DM+ +MSC group, where the outer diameter was (33.8±0.86) μm ($p=0.684$ *vs.* CG; $p=0.844$ *vs.* HFD+DM) (Figure 2A). According to the one-way ANOVA results, no statistically significant intergroup differences were found for this specific parameter (F-test, $p=0.447$).

Analysis of the HFD+DM group demonstrated the development of pronounced internal vascular remodeling, characterized by a critical narrowing of the arterial lumen (Figure 2B). The internal diameter of the arteries in this group significantly decreased to (18.9±1.23) μm, representing a 30.2% reduction compared to the control group (27.1±1.06) μm ($p<0.001$). Such structural narrowing under diabetic conditions indicates persistent angiospasm and the accumulation of extracellular matrix components within the vascular intima.

Parallel to the lumen narrowing, compensatory hypertrophy of the muscular coat (tunica media) was observed. In diabetic animals, the media thickness increased to (7.28±0.84) μm, which is more than double the values observed in the control group (3.51±0.22) μm ($p<0.001$). Density distribution plots (Figure 2C) clearly visualize a population shift of the vessels toward pathological wall thickening. The M/L ratio, also known as the Voganworth index, serves as a primary marker of vascular resistance. In the HFD+DM group, this index surged to (38.5±3.41) % (Figure 2D). Such a significant increase indicates a sharp decline in vascular wall elasticity and the establishment of persistent microcirculatory hypertension, which further exacerbates tissue ischemia in diabetic myopathy.

The administration of MSCs led to a significant attenuation of the observed vascular disorders. In the HFD+DM+MSC group, the internal diameter expanded to (22.8±1.16) μm ($p<0.001$ compared to the untreated diabetic group). Although this parameter did not fully return to the levels observed in healthy animals, such positive dynamics indicate a substantial restoration of vasodilatory capacity. Concurrently, cell therapy resulted in a reduction of media thickness to (5.53±0.46) μm, which was statistically significant compared to the HFD+DM group ($p<0.001$). This reduction suggests that MSCs possess the capacity to suppress the excessive proliferation of vascular smooth muscle cells (VSMCs), likely mediated through paracrine regulatory mechanisms and the modulation of the local cytokine profile.

The most dynamic changes were observed during the analysis of endothelial cells, which are the primary targets of chronic hyperglycemia. In the HFD+DM group, pronounced edema of the endothelial layer was detected. The endothelial cell height increased significantly to (2.46±0.17) μm, compared to (1.55±0.16) μm in the control group ($p<0.001$). These swollen cells protrude substantially into the vascular lumen, creating

Table 1: Morphometric parameters of rectus abdominis muscle arteries and endothelial cell characteristics in experimental groups.

Parameter	Control Group (n=10)	HFD+DM (n=10)	HFD+DM+MSC (n=10)
External diameter of arteries (μm)	34.2±1.07	33.5±1.04	33.8±0.86
Internal diameter (μm)	27.1±1.06	18.9±1.23***	22.8±1.16***, ###
Media thickness (μm)	3.51±0.22	7.28±0.84***	5.53±0.46***, ###
Media-to-lumen ratio (%)	12.9±1.11	38.5±3.41***	24.3±1.48***, ###
Endothelial cell height (μm)	1.55±0.16	2.46±0.17***	1.80±0.17**, ###
Nuclear-to-cytoplasmic ratio	0.31±0.02	0.20±0.02***	0.28±0.01**, ###
Relative volume of damaged endothelial cells (%)	2.28±0.23	31.60±3.40***	12.0±2.01***, ###

Note: Data are presented as mean±standard deviation (M±SD): * – $p<0.05$, ** – $p<0.01$, *** – $p<0.001$ compared to the Control group; # – $p<0.05$, ## – $p<0.01$, ### – $p<0.001$ compared to the HFD+DM group. Statistical significance was determined using one-way ANOVA followed by Tukey's HSD post-hoc test.

https://doi.org/10.46389/rjd-2026-2197

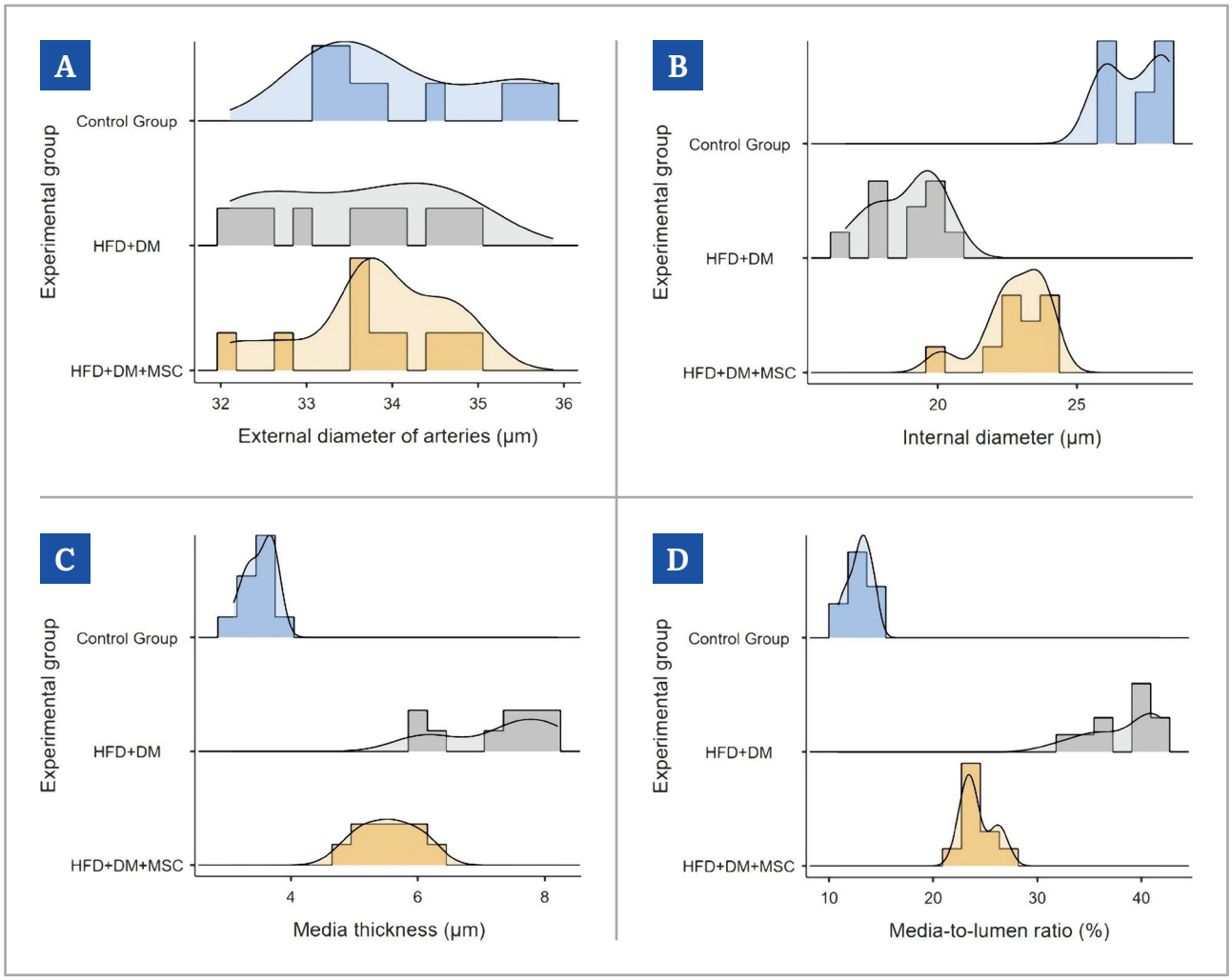

Figure 2: Distribution of morphometric parameters of the rectus abdominis muscle arteries across experimental groups: A – external diameter; B – internal diameter; C – media thickness; D – media-to-lumen ratio. Data are visualized using raincloud plots, showing individual data points, density distribution, and group trends.

additional mechanical resistance to blood flow. These morphological shifts were accompanied by a significant decrease in the nuclear-cytoplasmic ratio to (0.20±0.02) ($p<0.001$). Such a decrease in this index confirms that the expansion of cell volume occurs predominantly due to the cytoplasm, reflecting the development of vacuolization and hydropic degeneration (cellular edema) within the endothelial lining.

The therapeutic effect of MSCs was further evidenced by the stabilization of the endothelial barrier. In the treatment group (HFD+DM+MSC), the endothelial cell height decreased to (1.80±0.17) μm. Notably, the statistical significance of this reduction compared to the untreated diabetic group was $p=0.007$, highlighting the robust anti-edema effect of MSC therapy. Furthermore, the nuclear-cytoplasmic ratio in this group recovered to (0.28±0.01), indicating the normalization of intracellular metabolism and a marked reduction in cytoplasmic vacuolization (Figure 3A). These findings suggest that MSCs facilitate the structural repair of the endothelial lining, thereby restoring its functional integrity within the microcirculatory bed.

The assessment of the relative volume of damaged endothelial cells served as the most representative indicator of the severity of diabetic angiopathy. In the HFD+DM group, massive cellular damage was recorded, reaching (31.60±3.40) %. Nearly one in every three cells exhibited signs of irreversible destruction, including nuclear pyknosis, cytoplasmic fragmentation, and complete detachment from the basement membrane (desquamation). These structural alterations create a pro-thrombotic environment conducive to platelet adhesion and the progression of microthrombosis within the skeletal muscle vasculature.

The administration of MSCs resulted in a nearly threefold reduction in the volume of damaged

endothelium, decreasing it to (12.0±2.01) % ($p<0.001$). Visualization of these data using violin plots (Figure 3B) clearly demonstrates a significant shift in the cell population toward a healthy phenotype. Furthermore, the variability (spread of values) was markedly narrowed in the treatment group compared to the untreated diabetic group. Although the percentage of damaged cells remained higher than that of the control group (2.28±0.23) %, the substantial regenerative potential of MSCs confirms their potent angioprotective role. This recovery of the endothelial lining serves as a structural basis for the improved microcirculation and enhanced insulin sensitivity observed in the earlier functional tests.

In summary, the study results indicate that diabetes mellitus induces complex remodeling of the microvascular bed, characterized by a combination of medial hypertrophy and profound endothelial destruction. Systemic administration of MSCs effectively counteracts these pathological processes by alleviating endothelial cell edema, reducing the rate of cellular apoptosis, and promoting the restoration of the arterial lumen.

These quantitative findings strongly correlate with the histological evidence presented in the microphotographs (Figure 4), where the restoration of vascular wall integrity under the influence of cell therapy is clearly visualized. This structural recovery provides a morphological explanation for the metabolic improvements observed in the insulin tolerance tests.

Histological examination of the control group specimens revealed the typical architecture of the microvascular bed and skeletal muscle tissue (Figure 5). The small-caliber arteries of the rectus abdominis muscle were characterized by thin vascular walls with an organized arrangement of smooth muscle cells within the tunica media and a flattened morphology of the endothelial cells. The endomysium and interfibrillar spaces were minimal, showing no signs of edema or connective tissue disorganization. This histological profile served as the morphological baseline for the subsequent assessment of pathological changes in the diabetic group and the therapeutic efficacy of MSCs.

Discussion

The results of this study demonstrate a complex cascade of structural and metabolic impairments within the microcirculatory bed of skeletal muscles under diabetic conditions and highlight the multifaceted therapeutic potential of mesenchymal stem cells. Our findings not only verify the clinical efficacy of cell therapy but also provide deeper insights into the specific mechanisms of vascular remodeling associated with insulin resistance.

The development of systemic insulin resistance, as observed in the HFD+DM group via the ITT, represents a pivotal link in the pathogenesis of diabetic complications [14]. Current literature suggests that a high-fat diet triggers the activation of pro-inflammatory kinases, which subsequently impair insulin receptor signaling by inducing inhibitory phosphorylation of insulin receptor substrates [14, 15]. Our findings regarding the pathological glycemic curves strongly correlate with these established data, reinforcing the premise that skeletal muscle serves as the primary site for glucose disposal. Therefore, muscle-specific insulin resistance

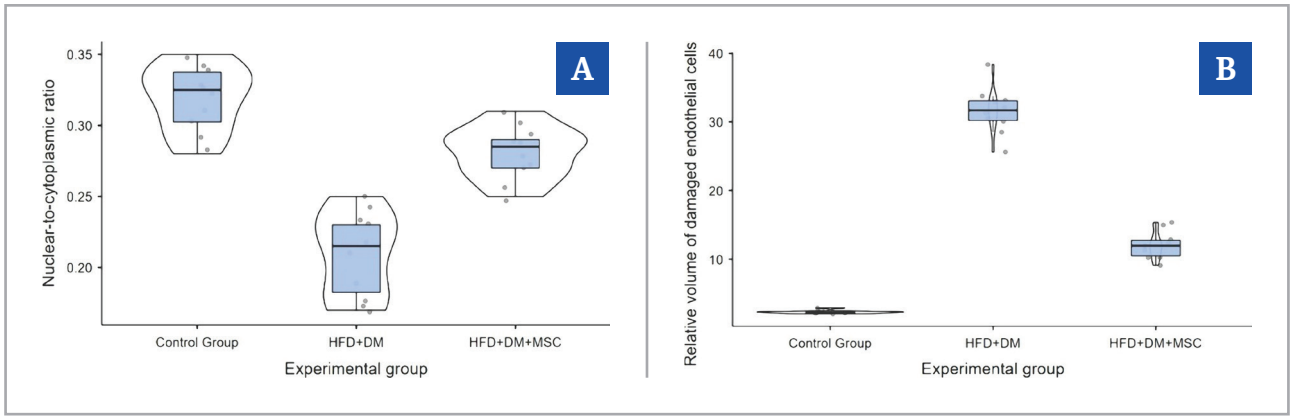

Figure 3: State of the endothelial lining in the rectus abdominis muscle arteries under experimental diabetes and MSC administration: A – nuclear-to-cytoplasmic ratio of endothelial cells; B – relative volume of damaged endothelial cells (%). Data are presented as box-and-whisker plots, where the central line represents the median, and individual points represent specific observations within each group. The violin contours indicate the distribution density of the data.

https://doi.org/10.46389/rjd-2026-2197

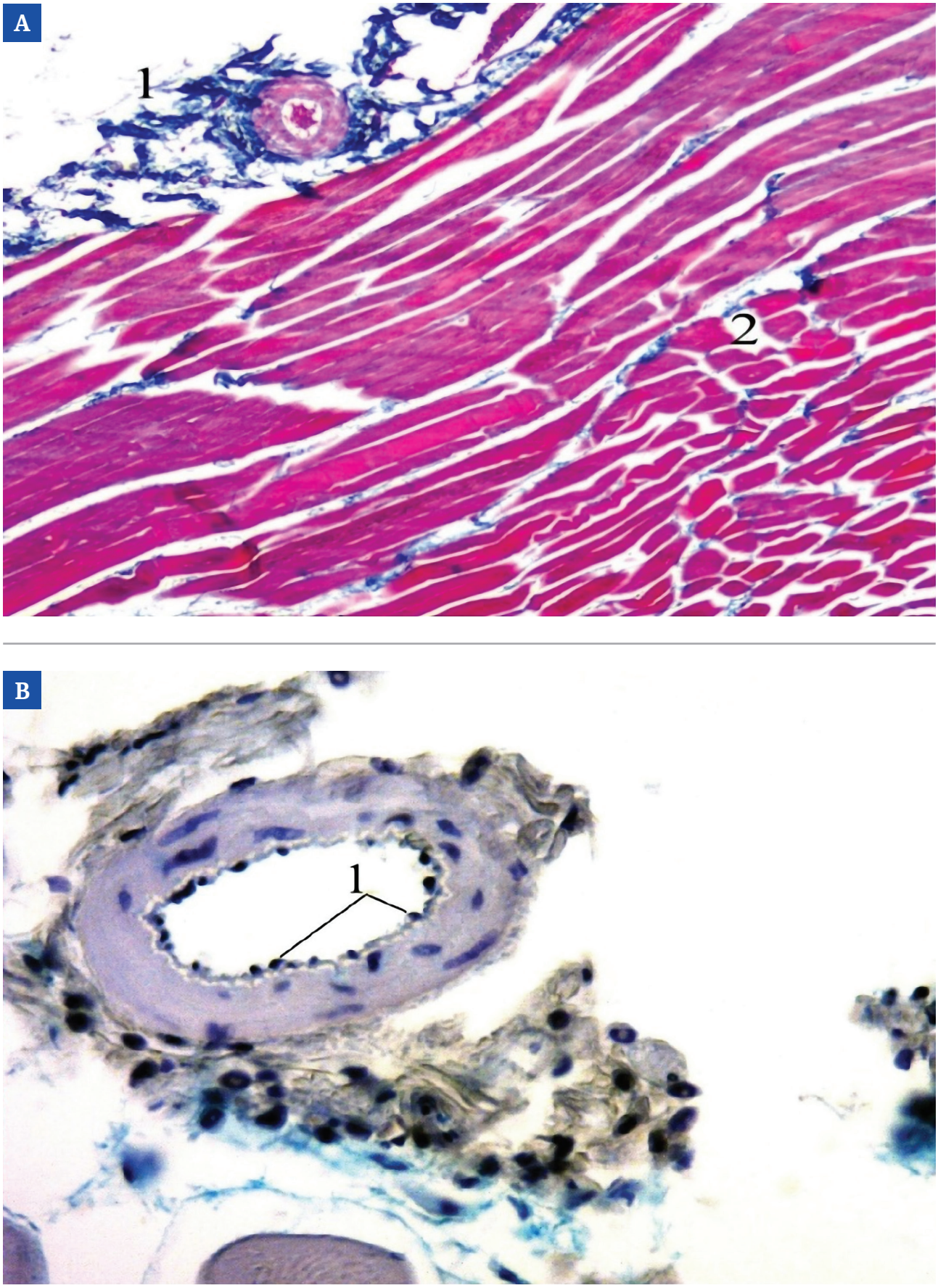

Figure 4: Morphology of the rectus abdominis muscle in experimental diabetes and MSC therapy. A – HFD+DM +MSC group: preserved skeletal muscle architecture (2) and ordered structure of the artery (1) within the perimysium. Masson's trichrome stain, 100x magnification. B – HFD+DM group (Diabetes): pronounced mucoid swelling of the arterial wall, deformation of edematous endothelial cells (1). Alcian Blue stain, 400x magnification.

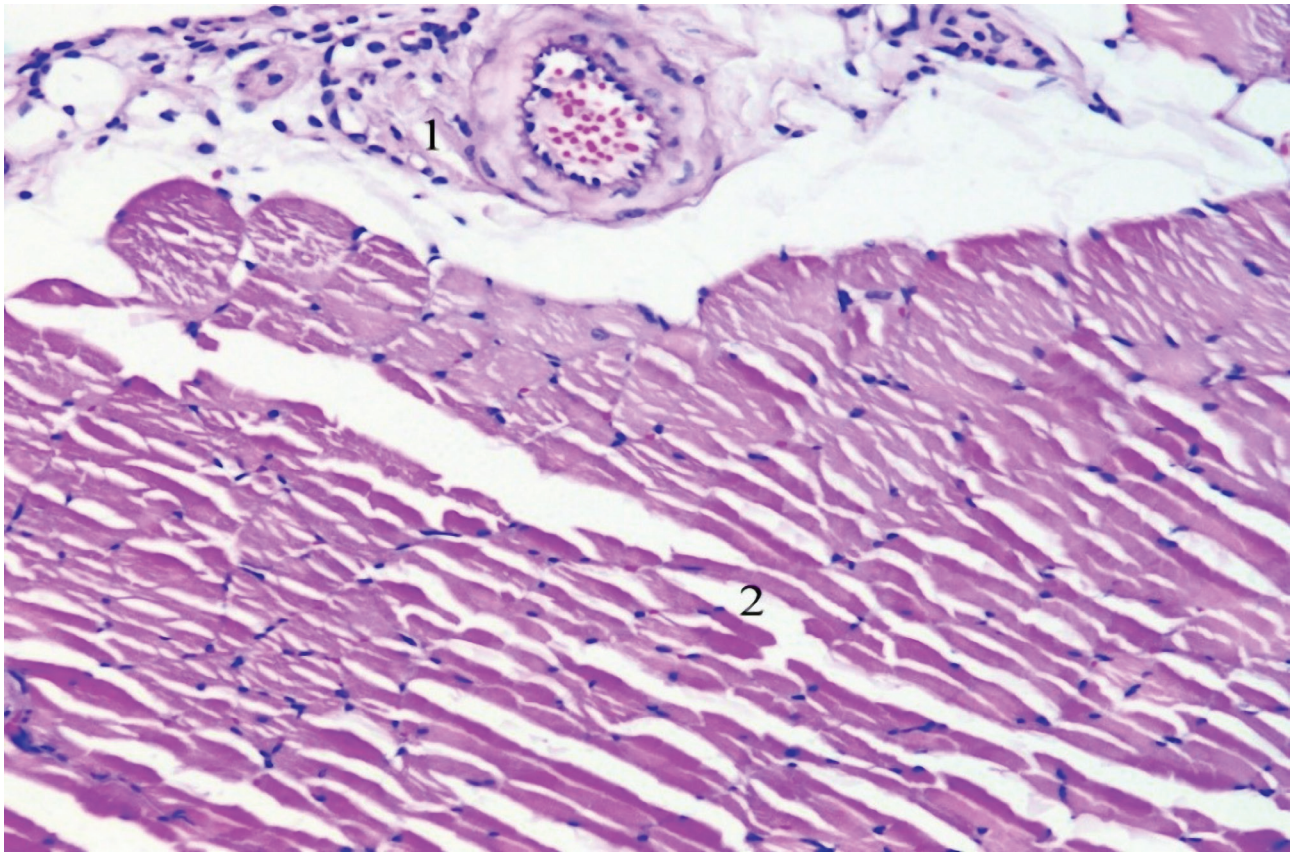

Figure 5: Normal histological architecture of the rectus abdominis muscle (Control group). The specimen demonstrates typical organization of the microcirculatory bed and skeletal muscle tissue. (1) muscular-type artery with a thin wall, organized smooth muscle cells in the media, and a wide, non-deformed lumen; (2) skeletal muscle fibers with peripheral nuclei and minimal endomysial space. Hematoxylin and eosin stain. Magnification ×200.

is a critical determinant of the overall metabolic prognosis in type 2 diabetes.

The improvement in ITT parameters following MSC administration in our study signifies a robust systemic metabolic effect. These findings align with recent reports indicating that MSCs secrete exosomes enriched with specific microRNAs that upregulate the expression of the GLUT4 glucose transporter in skeletal myocytes [16]. Consequently, MSCs should be viewed not merely as structural protectors but as active paracrine and endocrine modulators capable of neutralizing the "metabolic chaos" induced by a high-fat diet.

The central finding of our study was the dramatic increase in the Voganworth index to 38.5% in the diabetic group. This indicates hypertrophic vascular remodeling, which is considered the most prognostically unfavorable structural alteration of the microvasculature. Our data align with clinical evidence suggesting that an elevated M/L ratio in resistance arteries serves as an independent risk factor for major cardiovascular complications [17]. The observed twofold thickening of the tunica media (7.28±0.84) μm not only reduces the vessel's compliance but also creates a physical barrier that restricts the effective exchange of metabolites and hormones between the blood and the skeletal muscle interstitium.

Comparing our findings with existing literature, it can be argued that medial hypertrophy in diabetes is driven by the activation of the protein kinase C signaling pathway. This pathway stimulates the excessive production of extracellular matrix components, particularly type IV collagen and fibronectin. Our histological results, specifically Alcian blue staining, provide direct evidence of this process. The intense accumulation of acidic glycosaminoglycans within the arterial walls of the HFD+DM group indicates pronounced mucoid swelling of the connective tissue. Such "hyalinization" and structural disorganization of microvessels have been recognized in classical pathology as the definitive morphological substrate of diabetic angiopathy [18, 19].

The observed capacity of MSCs to reduce medial thickness and expand the vascular lumen (Figure 2) underscores their ability to modulate the phenotype of VSMCs. Our findings are consistent with reports

https://doi.org/10.46389/rjd-2026-2197

suggesting that MSC-derived paracrine factors facilitate a phenotypic switch in VSMCs, transitioning them from a proliferative (synthetic) state to a contractile phenotype [20]. Clinically, this modulation is manifested as a significant reduction in vascular wall stiffness and improved arterial compliance, which counteracts the progression of diabetic microangiopathy.

The assessment of the endothelium revealed pronounced hydropic dystrophy (cellular edema), accompanied by a critical reduction in the nuclear-cytoplasmic ratio. These morphological alterations are consistent with the dysfunction of Na+/K+-ATPase pumps, triggered by the chronic cellular energy deficiency characteristic of diabetes. The high prevalence of destructively altered endothelial cells (31.6%) observed in our study indicates a profound compromise of the blood-tissue barrier. Such extensive damage not only increases vascular permeability but also initiates a cascade of pro-inflammatory and pro-thrombotic events, further exacerbating the impaired microcirculation in skeletal muscles.

MSC therapy facilitated the stabilization of the endothelial layer (Figure 3), which is consistent with the "endothelial niche" hypothesis. According to this concept, MSCs selectively migrate to sites of vascular injury and secrete potent pro-survival factors, such as angiopoietin-1 and Vascular Endothelial Growth Factor A, which effectively prevent endothelial cell apoptosis. The application of complementary staining methods provided a comprehensive visualization of the microvascular pathology. Alcian blue staining revealed mucoid swelling, a direct consequence of plasmarrhagia – the leakage of plasma proteins and fluids into the vessel wall through the compromised endothelial barrier. This process, as documented in the literature, represents a critical stage in the development of diabetic hyalinosis [21], which our therapy was able to partially reverse or arrest.

Masson's trichrome staining in the MSC-treated group demonstrated a significant restoration of collagen homeostasis. In contrast to the chaotic interstitial fibrosis observed in untreated diabetic animals, an organized and ordered perimysium structure was restored following MSC administration. This structural improvement is critically important for muscle function, as excessive connective tissue fibrosis limits the mechanical extensibility of muscle fibers. Furthermore, the reduction of periarterial and interstitial collagen deposition lowers the physical resistance to oxygen diffusion, facilitating more efficient gas exchange between capillaries and myocytes. Consequently, the normalization of the connective tissue framework serves as a key factor in improving the functional state of the skeletal muscles under diabetic conditions.

Despite the fact that complete morphological recovery to the baseline levels of the control group was not achieved, the positive dynamics of key indices – specifically the Voganworth index and the volume of endothelial destruction – indicate that MSCs are capable of shifting the vascular system from a state of "destructive remodeling" to a state of "functional adaptation." This fundamental shift highlights the potential of cell therapy to arrest the progression of microvascular decay. Our findings pave the way for the development of novel cellular support protocols for patients suffering from diabetic angiopathy of the lower extremities and abdominal wall, potentially reducing the risk of ischemic complications and improving the quality of life in chronic diabetes.

Conclusions

Combined metabolic pathology (HFD+DM) induces persistent systemic insulin resistance and profound disorganization of the skeletal muscle microcirculatory bed. Systemic administration of MSCs provides effective metabolic correction, restoring peripheral insulin sensitivity and normalizing the glycemic profile, as evidenced by the insulin tolerance test at the 60th minute (6.69±0.68) mmol/L.

A key morphological marker of diabetic angiopathy in the rectus abdominis muscle is inward hypertrophic remodeling. In the diabetic group, the Voganworth index increased to (38.5±3.41) %, a threefold increase compared to the control group. MSC therapy effectively initiates reverse remodeling, significantly reducing media thickness to (5.53±0.46) μm and restoring arterial luminal diameter.

Chronic hyperglycemia triggers a cascade of destructive endothelial changes, including pronounced intracellular edema, increasing cell height to (2.46±0.17) μm and mucoid swelling. The destruction of (31.6±3.40) % of endothelial cells in the diabetic group signifies a critical breach of the blood-tissue barrier. MSC administration demonstrates a potent angioprotective effect, reducing endothelial destruction 2.6-fold.

Beyond vascular repair, cell therapy stabilizes the connective tissue framework of the muscle and reduces mucoid swelling. This restoration of the microenvironmental architecture provides the necessary

morphological basis for the regression of diabetic myopathy and improvement of muscle functional capacity.

Conflict of interest

The authors declare no conflict of interest.

References

1. Ogle GD, Wang F, Haynes A, Gregory GA, King TW, Deng K, Dabelea D, James S, Jenkins AJ, Li X, Ma RCW, Maahs DM, Oram RA, Pihoker C, Svensson J, Zhou Z, Magliano DJ, Maniam J. Global type 1 diabetes prevalence, incidence, and mortality estimates 2025: Results from the International diabetes Federation Atlas, 11th Edition, and the T1D Index Version 3.0. Diabetes Res Clin Pract. 2025 Jul;225:112277. doi: 10.1016/j.diabres.2025.112277.
2. Monaco CMF, Perry CGR, Hawke TJ. Diabetic Myopathy: current molecular understanding of this novel neuromuscular disorder. Curr Opin Neurol. 2017 Oct;30(5):545-552. doi: 10.1097/WCO.0000000000000479.
3. Hernández-Ochoa EO, Llanos P, Lanner JT. The Underlying Mechanisms of Diabetic Myopathy. J Diabetes Res. 2017;2017:7485738. doi: 10.1155/2017/7485738.
4. Mani AM, Dhanabalan K, Lamin V, Wong T, Singh MV, Dokun AO. BAG3 Attenuates Ischemia-Induced Skeletal Muscle Necroptosis in Diabetic Experimental Peripheral Artery Disease. Int J Mol Sci. 2022 Sep 14;23(18):10715. doi: 10.3390/ijms231810715.
5. Duan Y, Gao H, Su H, Liu A, Liu Y, Yuan H, Xie C. Exploring the Protective Effect of ShenQi Compound on Skeletal Muscle in Diabetic Macrovasculopathy Mice. Endocr Metab Immune Disord Drug Targets. 2020;20(6):943-951. doi: 10.2174/1871530320666200225094756.
6. Costa DN, Santosa S, Jensen MD. Sex differences in the metabolism of glucose and fatty acids by adipose tissue and skeletal muscle in humans. Physiol Rev. 2025 Jul 1;105(3):897-934. doi: 10.1152/physrev.00008.2024.
7. Kritsak M, Slabyi O, Gargula T, Yasinovskyi O, Levchyk O, Balitska O. Morphometric and structural changes in the rectus abdominis muscle of rats under conditions of experimental obesity and diabetes mellitus. RJDNMD. 2026 31Mar; 33(1):45-55. doi: 10.46389/rjd-2026-2183
8. Xu ZH, Chen JH, Huang FB, Lv GR. Evaluation of Skeletal Muscle Microcirculation and Reserve Function of the Type 2 Diabetes with Contrast-Enhanced Ultrasonography. Ultrasound Q. 2020 Mar;36(1):38-42. doi: 10.1097/RUQ.0000000000000459.
9. Hoffmann C, Weigert C. Skeletal Muscle as an Endocrine Organ: The Role of Myokines in Exercise Adaptations. Cold Spring Harb Perspect Med. 2017 Nov 1;7(11):a029793. doi: 10.1101/cshperspect.a029793.
10. Jehn P, Winterboer J, Kampmann A, Zimmerer R, Spalthoff S, Dittmann J, Gellrich NC, Tavassol F. Angiogenic effects of mesenchymal stem cells in combination with different scaffold materials. Microvasc Res. 2020 Jan;127:103925. doi: 10.1016/j.mvr.2019.103925.
11. Menezes K, Rosa BG, Freitas C, da Cruz AS, de Siqueira Santos R, Nascimento MA, Alves DVL, Bonamino M, Rossi MI, Borojevic R, Coelho-Sampaio T. Human mesenchymal stromal/stem cells recruit resident pericytes and induce blood vessels maturation to repair experimental spinal cord injury in rats. Sci Rep. 2020 Nov 11;10(1):19604. doi: 10.1038/s41598-020-76290-0.
12. Fischer UM, Harting MT, Jimenez F, Monzon-Posadas WO, Xue H, Savitz SI, Laine GA, Cox CS Jr. Pulmonary passage is a major obstacle for intravenous stem cell delivery: the pulmonary first-pass effect. Stem Cells Dev. 2009 Jun;18(5):683-92. doi: 10.1089/scd.2008.0253.
13. Nong Y, Guo Y, Tomlin A, Zhu X, Wysoczynski M, Li Q, Bolli R. Echocardiography-guided percutaneous left ventricular intracavitary injection as a cell delivery approach in infarcted mice. Mol Cell Biochem. 2021 May;476(5):2135-2148. doi: 10.1007/s11010-021-04077-6.
14. Gastaldelli A. Measuring and estimating insulin resistance in clinical and research settings. Obesity (Silver Spring). 2022 Aug;30(8):1549-1563. doi: 10.1002/oby.23503.
15. Gou Y, Liu B, Cheng M, Yamada T, Iida T, Wang S, Banno R, Koike T. d-Allulose Ameliorates Skeletal Muscle Insulin Resistance in High-Fat Diet-Fed Rats. Molecules. 2021 Oct 19;26(20):6310. doi: 10.3390/molecules26206310.
16. Cui J, Wang M, Zhang W, Sun J, Zhang Y, Zhao L, Hong Z, Li D, Huang YX, Zhang N, Chen Y. Enhancing insulin sensitivity in type 2 diabetes mellitus using apelin-loaded small extracellular vesicles from Wharton's jelly-derived mesenchymal stem cells: a novel therapeutic approach. Diabetol Metab Syndr. 2024 Apr 16;16(1):84. doi: 10.1186/s13098-024-01332-w.
17. Choi Y, Jacobs DR, Bancks MP, Lewis CE, Cha E, Yan F, Carnethon MR, Schreiner PJ, Duprez DA. Association of Cardiovascular Health Score With Early- and Later-Onset Diabetes and With Subsequent Vascular Complications of Diabetes. J Am Heart Assoc. 2023 Jan 3;12(1):e027558. doi: 10.1161/JAHA.122.027558.
18. Xiang H, Song R, Ouyang J, Zhu R, Shu Z, Liu Y, Wang X, Zhang D, Zhao J, Lu H. Organelle dynamics of endothelial mitochondria in diabetic angiopathy. Eur J Pharmacol. 2021 Mar 15;895:173865. doi: 10.1016/j.ejphar.2021.173865.
19. Faselis C, Katsimardou A, Imprialos K, Deligkaris P, Kallistratos M, Dimitriadis K. Microvascular Complications of Type 2 Diabetes Mellitus. Curr Vasc Pharmacol. 2020;18(2):117-124. doi: 10.2174/1570161117666190502103733.
20. Chen PY, Qin L, Li G, Malagon-Lopez J, Wang Z, Bergaya S, Gujja S, Caulk AW, Murtada SI, Zhang X, Zhuang ZW, Rao DA, Wang G, Tobiasova Z, Jiang B, Montgomery RR, Sun L, Sun H, Fisher EA, Gulcher JR, Fernandez-Hernando C, Humphrey JD, Tellides G, Chittenden TW, Simons M. Smooth Muscle Cell Reprogramming in Aortic Aneurysms. Cell Stem Cell. 2020 Apr 2;26(4):542-557.e11. doi: 10.1016/j.stem.2020.02.013.
21. Moriya T, Omura K, Matsubara M, Yoshida Y, Hayama K, Ouchi M. Arteriolar Hyalinosis Predicts Increase in Albuminuria and GFR Decline in Normo- and Microalbuminuric Japanese Patients With Type 2 Diabetes. Diabetes Care. 2017 Oct;40(10):1373-1378. doi: 10.2337/dc17-0209.

 https://doi.org/10.46389/rjd-2026-2197